AMERICAN SOCIETY FOR MICROBIOLOGY | Journal of Virology®

VIRUS-CELL INTERACTIONS

Cellular and Viral Determinants of Herpes Simplex Virus 1 Entry and Intracellular Transport toward the Nuclei of Infected Cells

Farhana Musarrat,[a,b] Vladimir Chouljenko,[a,b] Konstantin G. Kousoulas[a,b]

[a]Division of Biotechnology and Molecular Medicine, School of Veterinary Medicine, Louisiana State University, Baton Rouge, Louisiana, USA
[b]Department of Pathobiological Sciences, School of Veterinary Medicine, Louisiana State University, Baton Rouge, Louisiana, USA

ABSTRACT Herpes simplex virus 1 (HSV-1) employs cellular motor proteins and modulates kinase pathways to facilitate intracellular virion capsid transport. Previously, we and others have shown that the Akt inhibitor miltefosine inhibited virus entry. Herein, we show that the protein kinase C inhibitors staurosporine (STS) and Gouml inhibited HSV-1 entry into Vero cells and that miltefosine prevents HSV-1 capsid transport toward the nucleus. We have reported that the HSV-1 UL37 tegument protein interacts with the dynein motor complex during virus entry and virion egress, while others have shown that the UL37/UL36 protein complex binds dynein and kinesin, causing a saltatory movement of capsids in neuronal axons. Coimmunoprecipitation experiments confirmed previous findings from our laboratory that the UL37 protein interacted with the dynein intermediate chain (DIC) at early times postinfection. This UL37-DIC interaction was concurrent with DIC phosphorylation in infected, but not mock-infected, cells. Miltefosine inhibited dynein phosphorylation when added before, but not after, virus entry. Inhibition of expression of motor accessory protein dynactins (DCTN2 and DCTN3) and the adaptor proteins end binding protein (EB1) and bicaudal D homolog 2 (BICD2) using lentiviruses expressing specific short hairpin RNAs (shRNAs) inhibited intracellular transport of virion capsids toward the nucleus of human neuroblastoma (SK-N-SH) cells. Coimmunoprecipitation experiments revealed that the major capsid protein Vp5 interacted with dynactins (DCTN1/p150 and DCTN4/p62) and the end binding protein (EB1) at early times postinfection. These results show that Akt and kinase C are involved in virus entry and intracellular transport of virion capsids, but not in dynein activation via phosphorylation. Importantly, both the UL37 and Vp5 viral proteins are involved in dynein-dependent transport of virion capsids to the nuclei of infected cells.

IMPORTANCE Herpes simplex virus 1 viruses enter either via fusion at the plasma membranes or endocytosis depositing the virion capsids into the cytoplasm of infected cells. The viral capsids utilize the dynein motor complex to move toward the nuclei of infected cells by using the microtubular network. This work shows that inhibitors of the Akt kinase and kinase C inhibit not only viral entry into cells but also virion capsid transport toward the nucleus. In addition, the work reveals that the virion protein ICP5 (VP5) interacts with the dynein cofactor dynactin, while the UL37 protein interacts with the dynein intermediate chain (DIC). Importantly, neither Akt nor kinase C was found to be responsible for phosphorylation/activation of dynein, indicating that other cellular or viral kinases may be involved.

KEYWORDS Akt, HSV-1, intracellular transport, PKC, SK-N-SH cells, dynein, motor protein complex, protein kinases, viral entry, viral-cellular protein interaction

Intracellular transport is mediated by the cytoskeleton network and motor proteins within the cytoplasm of cells. Short-distance movement of cargo is mediated by actin and myosin, while long-distance transport (>1 μm) of organelles and other cargo requires ATP-dependent motor proteins and accessory factors, which are transported

Citation Musarrat F, Chouljenko V, Kousoulas KG. 2021. Cellular and viral determinants of herpes simplex virus 1 entry and intracellular transport toward the nuclei of infected cells. J Virol 95:e02434-20. https://doi.org/10.1128/JVI.02434-20.

Editor Richard M. Longnecker, Northwestern University

Address correspondence to Konstantin G. Kousoulas, vtgusk@lsu.edu.

Received 25 December 2020
Accepted 8 January 2021
Accepted manuscript posted online 20 January 2021
Published 10 March 2021

via the microtubule network (1–4). The plus end or the growing end of the microtubule is located toward the periphery (cell membrane) of the cell and helps in cell growth and migration. Several end binding microtubule-associated proteins (MAPs) and plus-tip-interacting proteins (TIPs) facilitate intracellular transport (5). Specifically, the end binding protein (EB1) recognizes the growing end of a dynamic microtubule, recruits other MAPs, and facilitates binding of intracellular cargoes and organelles to the microtubular network for intracellular transport (6–8). The minus end of the microtubule is proximal to the nucleus and the microtubule organizing center (MTOC). The two major motor proteins dynein and kinesin mediate intracellular cargo transport toward the nucleus and cell periphery, respectively. Dynein is a multisubunit complex, with each subunit having a distinct function. The heavy chains possess ATPase activity, which is required for movement along the microtubules. The intermediate chain (IC) and light chain (LC) regulate motor activity and mediate interactions with other cofactors and cargo (9–15). A number of different accessory proteins interact with the dynein motor complex and modulate dynein-dependent transport. Dynactin (DCTN) is a large molecule consisting of several components, namely, DCTN1 (p150), DCTN2 (dynamitin/p50), DCTN3 (p24/22), DCTN4 (p62), DCTN5 (p25), DCTN6 (p27), CapZ, and the Arp polymer. One end of DCTN1 (p150) binds to the dynein IC, and the other end is associated with microtubules. DCTN4 (P62), Arp polymer, and CapZ participate in cargo binding (16–19). The bicaudal D homolog (BICD) facilitates dynein-dependent transport in epithelial and neuronal cells (20–22). BICD2 binds to DCTN2 (p50), docks on the Arp polymer, and helps in the recruitment of dynein cargo (23). BICD2 also interacts with the N terminus of the dynein heavy chain and the light intermediate chain, which together enhance dynein-dynactin interactions (15). In addition, BICD2 is associated with the cellular transport of mRNA and organelles and helps to position the nucleus during cell division by docking at the nuclear pore (24).

Viruses hijack dynein-dependent intracellular cargo transport to facilitate infection. Several viruses have been shown to utilize the cellular motor protein dynein to facilitate intracellular virion transport (25–30). Herpes simplex virus 1 (HSV-1) capsids take advantage of cellular intracellular transport mechanisms to travel along cellular microtubules toward the cell nucleus where it delivers its genome for replication (7, 31–34). Although most of the outer tegument proteins of HSV-1 dissociate in the cytoplasm following entry into host cells, the tegument proteins UL36, UL37, and US3 remain attached to the capsid during intracellular transport to the nucleus and are known to be involved in intracellular capsid transport (31, 33, 35–42). The HSV-1 inner tegument proteins UL36 and UL37 interact with the cellular motor proteins kinesin and dynein, respectively. These interactions have been suggested to cause bidirectional or saltatory movement along microtubules (31, 32, 36, 43, 44). In some cases, virus transport occurs at the expense of cellular transport. HSV-1 infection disrupts mitochondrial transport by altering kinesin-mediated motility (28). For pseudorabies virus (PRV), VP1/2 (UL36 homolog) interacts with the dynein intermediate chain (DIC) and dynactin (p150) in the HEK293 cell line, while VP1/2 alone was shown to move cargo via the microtubule network. The proline-rich sequence of VP1/2 appears to play an essential role in the retrograde transport of PRV in neuronal cultures and *in vivo* (45). Similar roles have been suggested for a phosphoprotein specified by pseudorabies virus and lyssavirus, which bind to the dynein light chain 8 (LC8). Small interfering RNA (siRNA)-mediated depletion of the dynein heavy chain DYNC1H1 inhibited human immunodeficiency virus (HIV) infection, although siRNA depletion of other dynein components had little to no effect on HIV infection in TZM-bl cells (24). The dynein light chain 2 (DLC-2) transports HIV integrase, and DLC-1 interacts with HIV capsid and affects reverse transcription (46). HIV-1 exploits one or more dynein adaptors for efficient infection and transport toward the nucleus (47). Dynein adaptor BICD2, dynactin components DCTN2, DCTN3, and ACTR1A (Arp1 rod) were essential for HIV permissiveness in TZM-bl cells (24). The adenovirus hexon protein directly recruits the intermediate dynein chain (DIC) for capsid transport (48). Interestingly, dynein interaction with the simian virus 40 (SV40) virion after entry into cells causes a disassembly of the virion

that is required for transport toward the nucleus (30). The tegument protein ppUL32 of human cytomegalovirus (HCMV) interacts with BICD1, and its depletion resulted in low virus yield due to insufficient trafficking of ppUL32 to the cytoplasmic viral assembly compartment (AC) (22). The end binding protein 1 (EB1) is essential for HSV-1 infection, and the microtubule plus-end-associated protein CLIP 170 initiates HSV-1 retrograde transport in primary human cells (7).

Regulation of intracellular transport by kinases. Intracellular transport is regulated by various protein kinases through direct posttranslational modification (phosphorylation) of motors, accessory proteins, cargoes, or via indirect modification of the microtubular network (49–57). Mitogen-activated protein kinases (MAPKs) play a pivotal role in anterograde transport of neurofilament in differentiated neuroblastoma cells, and inhibition of MAPKs completely inhibits transport and organization of neurofilament in axonal neurites (58). The kinase Akt (protein kinase B) is involved in transport of synaptic vesicles, as shown by brain-derived neurotrophic factor (BDNF)- and amyloid precursor protein (APP)-containing secretory vesicles in cortical neurons (59). Protein kinase C (PKC) is involved in actin cytoskeleton modification in retinal bipolar cells and controls vesicular transport in primary human macrophages (54, 56). Also, PKC regulates intracellular organelle transport in sensory and sympathetic neurons. Activation of PKC and caspases by neurotoxin in dopaminergic neurons affects fast axonal transport, a phenomenon observed in Parkinson's disease. In mice, PKC activation leads to inhibition of neurotrophin retrograde transport to the trigeminal ganglia and superior cervical ganglia when a PKC activator is injected in the eye (57, 60, 61). Some kinases directly modify motor proteins. Specifically, inhibition of glycogen synthase kinase (GSK3β) enhances retrograde motility by direct phosphorylation of dynein intermediate chain (DIC) (62). GSK3β also recruits EB1 to the plus end of microtubules, which is important for the loading of cargo and virions on the microtubular network (63).

Modulation of cellular kinases involved in intracellular transport by viruses. Modification of cellular kinases is another way that viruses regulate intracellular transport. HSV-1 activates the serine-threonine kinase (Akt) (64) and mitogen-activating protein kinases (MAPKs) at later times postentry (65). The phosphatidylinositol 3-kinase (PI3K)/Akt pathway is activated following HIV Env-CD4 mediated fusion. HIV requires PI3K p110α/PTEN signaling during entry into T cells, PM1 cells, and TZM-b1 cells (66). Inhibition of certain cellular kinases prevents HSV-1 entry and transport toward the nucleus. Specifically, Akt inhibition by miltefosine inhibits HSV-1 (McKrae) entry into Vero and SK-N-SH cells (67). Also, PI3K inhibition inhibits HSV-containing endosome trafficking (68). Some viruses modify the motor proteins via activation of kinases for their transport in the cytoplasm. Adenovirus activates protein kinase A (PKA) and p38 MAPK and is involved in phosphorylation of the dynein light intermediate chain 1 (LIC-1), which subsequently binds the adenovirus hexon (69). Adenoviral activation of kinases enhances the nuclear targeting, possibly through integrins (70).

In this report, we investigate the role of cellular kinases and motor proteins in HSV-1 intracellular transport. Previously, we reported that Akt is necessary for HSV-1 entry into cells (67). Herein, we show that the broad-spectrum Akt and PKC inhibitor miltefosine prevented HSV-1 entry and intracellular transport of HSV-1 capsids after virus entry into cells. We show that HSV-1 infection activates dynein by phosphorylating the intermediate chain (DIC) at an early time postinfection independently of PKC or Akt activation via phosphorylation. Furthermore, we show that the HSV-1 tegument protein UL37 interacts with the intermediate chain of cellular motor protein dynein (DIC) and that capsid protein VP5 (ICP5) interacts with motor accessory proteins dynactin (DCTN1/p150, DCTN4/p62), EB1 but not DIC during intracellular capsid transport toward the nucleus. These results suggest that HSV-1 modulates both virus entry and intracellular transport through specific protein-protein interactions and modulation of cellular kinases.

RESULTS

Akt is required for HSV-1 (McKrae) intracellular capsid transport toward the nucleus. Previously, we showed that Akt inhibition blocke HSV-1 (McKrae) entry into epithelial and neuroblastoma cells (67). To determine if Akt has a role in intracellular transport of HSV-1, SK-N-SH cells were treated with the Akt inhibitor miltefosine at different concentrations (10, 30, 50, and 70 μM) at 37°C and intracellular transport was monitored by immunofluorescence microscopy. Before drug treatment, cells were infected with HSV-1 (McKrae) (multiplicity of infection [MOI] of 20) for 1 h at 4°C and then shifted to 37°C for 15 min to allow virus entry into cells. Following a wash with low-pH buffer, cells were incubated with the inhibitors for 5 h and subsequently were processed for visualization of the ICP5 (Vp5)-containing capsids by immunofluorescence. HSV-1 (McKrae) virions were transported toward the nucleus of infected cells resulting in productive infection, as evidenced by the expression of the ICP5 protein (red) inside the nucleus (blue) at 5 h postinfection (hpi). However, viral capsids remained in the periphery of the cytoplasm in miltofesine-treated cells (Fig. 1A). At 15 min postinfection, the relative locations of virion capsids detected were similar between no-drug-treated and Akt-treated cells quantified by determining the average fluorescent signal per cell. In the presence of Akt, the fluorescence signals remained similar to the 15-min time points for the Akt-treated cells (Fig. 1B).

Protein kinase C is required for HSV-1 (McKrae) entry. Our previous results indicated that the serine-threonine kinase Akt was required for HSV-1 entry into cells. Miltefosine blocks both Akt and PKC enzymatic activities. Therefore, we investigated the specific role of PKC in HSV-1 entry and transport in Vero cells. Staurosporine (STS) is a broad-spectrum protein kinase inhibitor. It inhibits protein kinase C, protein kinase A, p60v-src tyrosine protein kinase, and CaM kinase II at different concentrations. Gouml is a potent, fast-acting, and specific PKC inhibitor of different PKC subtypes, such as PKCα, PKCβ, PKCγ, PKCδ, PKCζ and PKCμ. Treatment with either Gouml or staurosporine for 4 h at 37°C caused a dose-dependent reduction in the entry of HSV-1 (McKrae) (100 PFU) in Vero cells. Maximum inhibition was observed at concentrations of 90 μM (Gouml) and 0.5 μM (STS), respectively (Fig. 2A). Detection of the VP5-containing capsids via immunofluorescence revealed drastic reduction of capsids in the cytoplasm of infected cells (Fig. 2B). This reduction was the combined effect of these inhibitors in blocking both virus entry and intracellular capsid transport, since the incubation of infected cells for 4 h at 37°C dislodged virions bound to cell surfaces, but unable to enter (data not shown).

HSV-1 (McKrae) activates the dynein intermediate chain. Previously, it was shown that HSV-1 tegument proteins bind both plus- and minus-end-directed motor proteins simultaneously, while moving along the microtubules (35, 36, 71). To determine if HSV-1 infection results in the modification of the dynein motor during intracellular transport, Vero cells were infected with HSV-1 (McKrae), and infected cell lysates prepared at different times postinfection were analyzed for dynein phosphorylation. HSV-1 infection caused phosphorylation of the intermediate dynein chain 1B as early as 15 min postinfection (Fig. 3A). An increase in the level of phosphorylation was observed from 15 min to 3 h postinfection, which is approximately the time that it takes for HSV-1 capsids to be transported to the nucleus of infected cells (68).

Dynein phosphorylation/activation by HSV-1 (McKrae) is independent of either Akt or PKC signaling. Previously, we and others have reported that HSV-1 activated the Akt pathway at early times postinfection (64). We considered that the Akt/PKC pathway is upstream of dynein activation and plays a role in activating dynein for the capsid motility. To investigate if HSV-1 (McKrae) activates/phosphorylates dynein via the Akt/PKC pathway, miltefosine was used to treat cells before and after virus entry, and the resultant dynein phosphorylation pattern was monitored at 1 h postinfection. Miltefosine inhibited dynein phosphorylation at concentrations of 75 and 100 μM (Fig. 3B and D), which we reported to inhibit virus entry previously (67). However, once the virus entered the cell, blocking Akt or PKC did not inhibit activation of dynein by HSV-1 (McKrae) (Fig. 3C), but inhibited intracellular capsid transport (Fig. 1 and 2B).

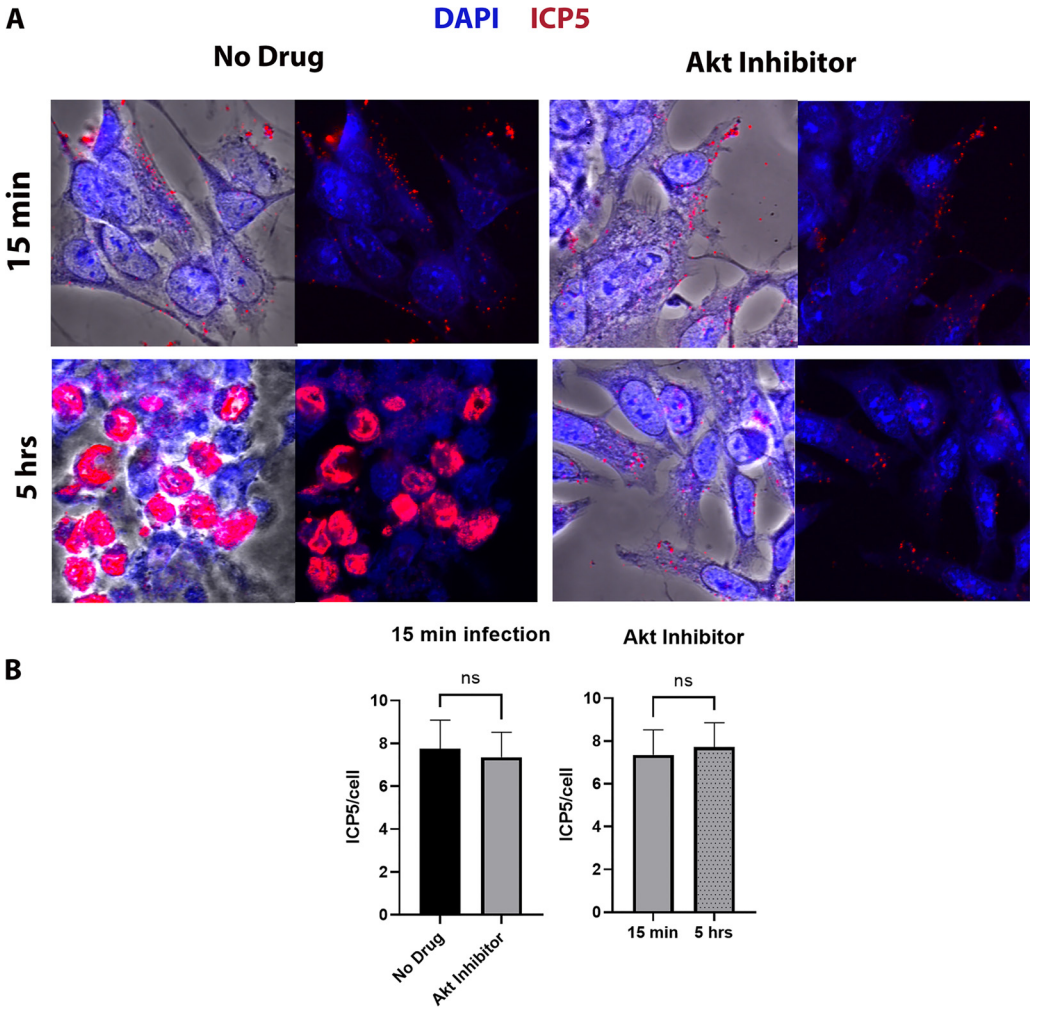

FIG 1 Effect of Akt HSV-1 transport. (A) SK-N-SH cells were adsorbed at 4°C with HSV-1 (McKrae) at an MOI of 20 for 1 h, shifted to 37°C for 15 min, and then washed with low-pH buffer. The Akt inhibitor miltefosine was added at a concentration of 30 μM, and the mixture was incubated for 5 h at 37°C. The 8-well chamber slide was then fixed with formalin, permeabilized with methanol, and prepared for fluorescence microscopy. Antibody against VP5 (ICP5) (red) was used, and nuclei were stained with DAPI (blue). Capsids colocalized in the nuclei appear purple. Magnification is 63× under oil immersion. (B) The amount of fluorescence detected with the anti-ICP5 antibody (virion capsids) was quantified by fluorescence imaging of 10 different random sections of slides, using ImageJ software. The fluorescence signals per cell were counted, and their average value was used to plot the graph. Statistical comparison was conducted by Graph Pad Prism using Student's *t* test. Error bars represent the 95% confidence interval about the mean. Differences were determined significant at $P < 0.05$.

Motor accessory proteins are essential for HSV-1 (McKrae) intracellular transport. To determine the role of motor proteins and adaptors in virion capsid intracellular transport toward the nucleus, we generated several SK-N-SH knockdown cell lines using lentivirus-based expression of specific shRNAs (Santa Cruz, Inc.). We used commercial shRNAs targeting dynein heavy chain (DHC), dynactin 2 (DCTN2), dynactin 3 (DCTN3), end binding protein 1 (EB1), and BICD2. GFP control shRNA was used to determine the efficiency of lentiviral infection for each cell line. The plasmid vector also contains the puromycin resistance gene for positive clone selection. A toxicity test for puromycin was performed for SK-N-SH cell lines, and 10 μg/ml was found sufficient for selecting knocked-down cells in the SK-N-SH cell line (Fig. 4A). A serial passage of all SK-N-SH cells up to 10 passages did not cause significant cellular toxicity or significant replication issues. However, we observed increasing changes in morphology and viability after 10 passages, with loss of cells at approximately 20 passages. Therefore, all experiments performed in this study were limited to cell lines at early passages (<5).

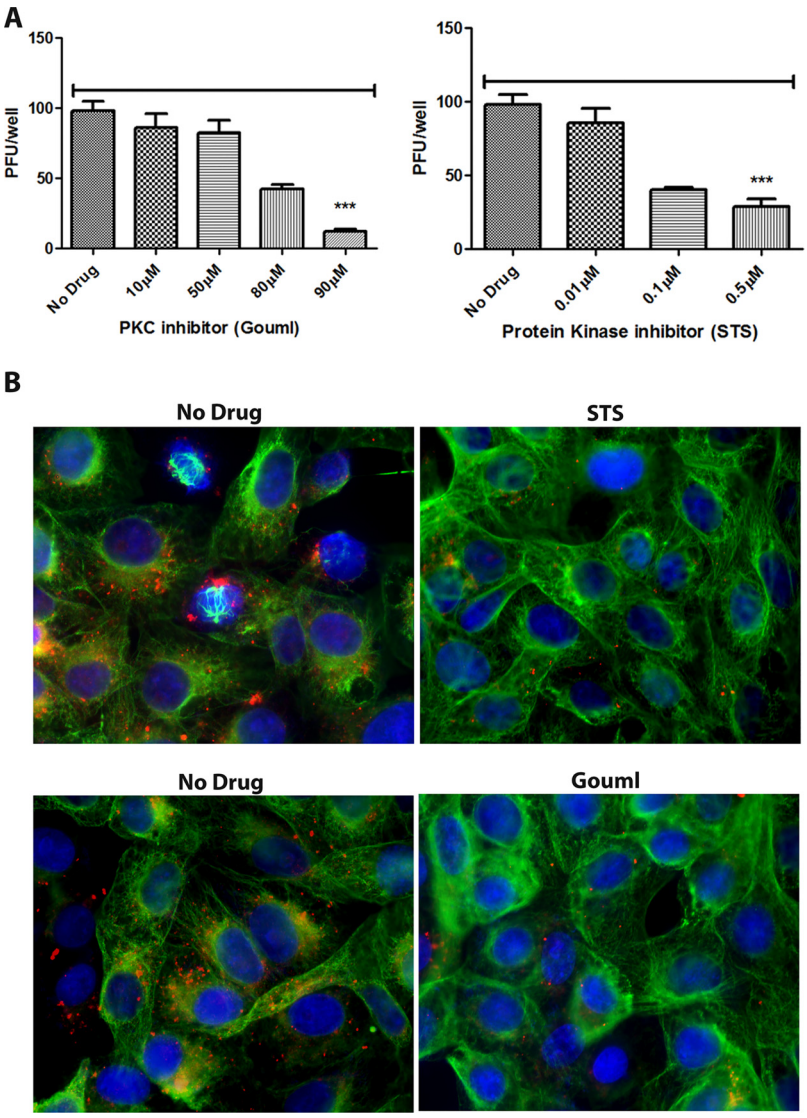

FIG 2 Effect of PKC inhibitors on HSV-1 entry. (A) Vero cells were treated with a series of dilutions of the PKC inhibitor Gouml or the protein kinase inhibitor staurosporine (STS) for 4 h and then infected with HSV-1 (McKrae) (100 PFU) for 1 h at 4°C. Cells were incubated at 37°C for 48 h for plaque assay. Viral plaques were counted after crystal violet staining. ***, $P < 0.001$ versus no-drug-treated control. Statistical comparison was conducted by Graph Pad prism using ANOVA with a *post hoc t* test with Bonferroni adjustment. Error bars represent the 95% confidence interval about the mean. (B) Vero cells were treated with a series of dilutions of PKC inhibitor (Gouml) or protein kinase inhibitor (staurosporine) for 4 h and then infected with McKrae (MOI of 20) for 1 h at 4°C. Cells were incubated at 37°C for 3 h and then fixed with formalin and permeabilized with methanol. Antibodies against VP5 (ICP5) (red), and α-tubulin (green) were used, and nuclei were stained with DAPI (blue). Magnification, 40×.

Cellular extracts from the engineered cell lines were prepared, and the level of BICD2, EB1, DCTN2, an DCTN3 expression was assessed via Western immunoblots. All cell lines showed highly significant reduction of the targeted proteins in comparison to the control shRNA-treated lysates (Fig. 4B).

We investigated HSV-1 (McKrae) intracellular transport in the EB1, BICD2, DCTN2, DCTN3, and DHC knockdown SK-N-SH cells by detecting the major protein VP5 (ICP5) at early times postinfection via indirect immunofluorescence assay (IFA). The SK-N-SH dynein heavy-chain knockdown cells did not survive and thus were not used in these experiments. Control cells were selected using the same process as with the knockdown cell lines, except that a control (scrambled) shRNA was used. Following adsorption of the

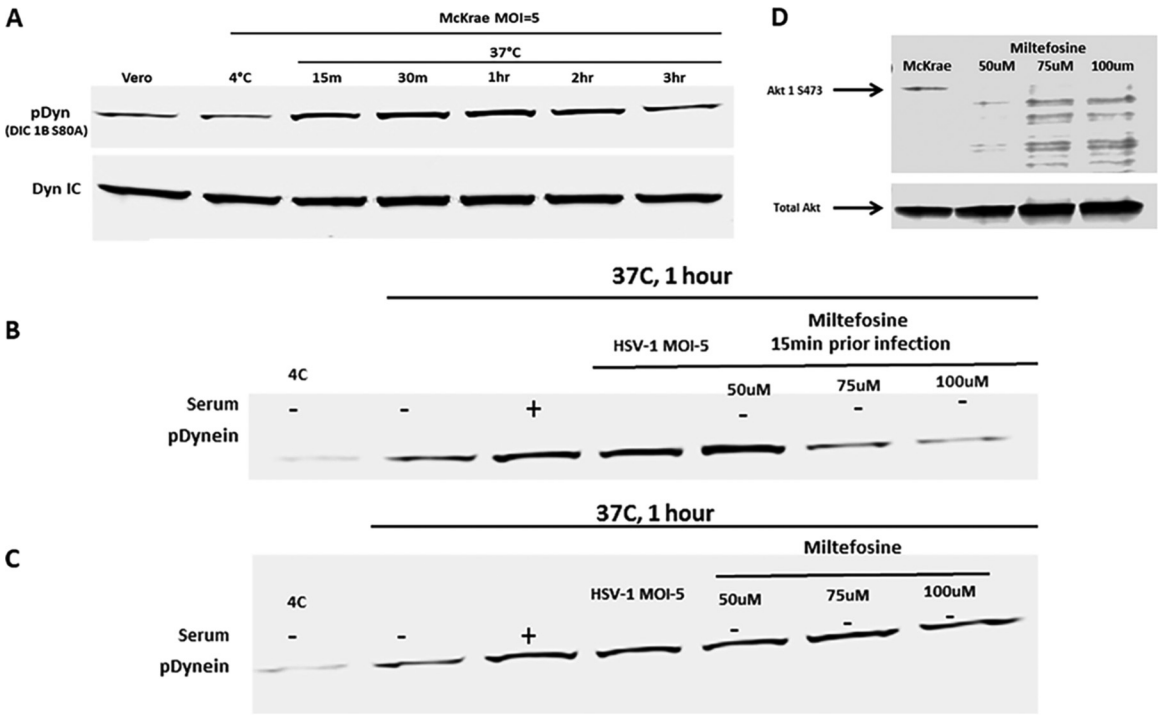

FIG 3 Dynein activation by HSV-1. (A) Serum-starved Vero cells were infected with HSV-1 (McKrae) at 4°C for 1 h at an MOI of 5 and then shifted to 37°C for 15 min, 30 min, 1 h, 2 h, and 3 h. Cells were lysed with the NP-40 lysis buffer containing a protease inhibitor cocktail and analyzed for phosphorylated dynein intermediate chain (DIC 1B S80A) by SDS-PAGE. The total dynein intermediate chain (DIC) protein was used as the loading control. (B) Vero cells were pretreated with miltefosine at 37°C. Cells were infected with HSV-1 (McKrae) at 4°C for 1 h at an MOI of 5 and then shifted to 37°C for 1 h. Cells were lysed with NP-40 lysis buffer containing a protease inhibitor cocktail and analyzed for the presence of the phosphorylated dynein intermediate chain (DIC 1B S80A) by SDS-PAGE. (C) Following infection with HSV-1 (McKrae) at 4°C for 1 h at an MOI of 5, cells were incubated at 37°C for 15 min, and then miltefosine was added and the mixture was incubated for 1 h. Cell lysates were prepared the same way for SDS-PAGE analysis. + and − indicate whether serum was added (+) or not (−). (D) Effect of miltefosine on Akt phosphorylation. Total Akt was used as loading control.

virus at 4°C for an hour, control cells were incubated at 37°C for 30 min, 3 h, and 5 h to observe the time required for the virus to travel toward the nucleus. VP5 (ICP5)-stained virions at 30 min after infection were observed predominantly in the periphery of cells. At 3 hpi, capsids were detected in the cytoplasm and proximal to the nuclear membranes. At 5 hpi, VP5 (ICP5) was detected within the nucleus, representing newly expressed VP5 (ICP5) (Fig. 5A). We considered that the distinct VP5 puncta originated from intact input capsids, while diffuse VP5 fluorescence signals originated from newly synthesized VP5 that is expressed in the cytoplasm and migrates into the nuclei, where virion capsids are assembled. There was a marked reduction in the major capsid protein VP5 (ICP5) detected in the nucleus in EB1, BICD2, DCTN2, and DCTN3 knockdown infected SK-N-SH cells at 5 hpi compared to the control shRNA-treated SK-N-SH cells (Fig. 5B). Viral capsids were mostly localized near the plasma membrane for the DCTN2 and DCTN3 knockdown cells. In the BICD2 and EB1 knockdown cells, virion capsids appeared to be localized in the cytoplasm and nuclear periphery (Fig. 5B). Transmission electron microscopy was performed on EB1, BICD2, DCTN2, and DCTN3 knockdown infected cells. Aggregation of capsid like structures was visible in the nucleus of the control shRNA-treated cells after 5 hpi. However, HSV-1 viral capsids were not observed in the nucleus of cells treated with EB1 shRNA, BICD2 shRNA, DCTN2 shRNA, or DCTN3 shRNA. Instead, capsids were mostly seen near the cell membrane and in the cytoplasm of infected SK-N-SH knockdown cells, consistent with the IFA results (Fig. 6).

HSV-1 tegument protein UL37 and capsid protein VP5 interact with cellular motor accessory proteins during intracellular transport. Previously, it was shown that the HSV-1 capsid interacted with EB1 and dynein and that the tegument proteins UL37/UL36 associated with dynein and kinesin motors during virion egress (30, 32, 35,

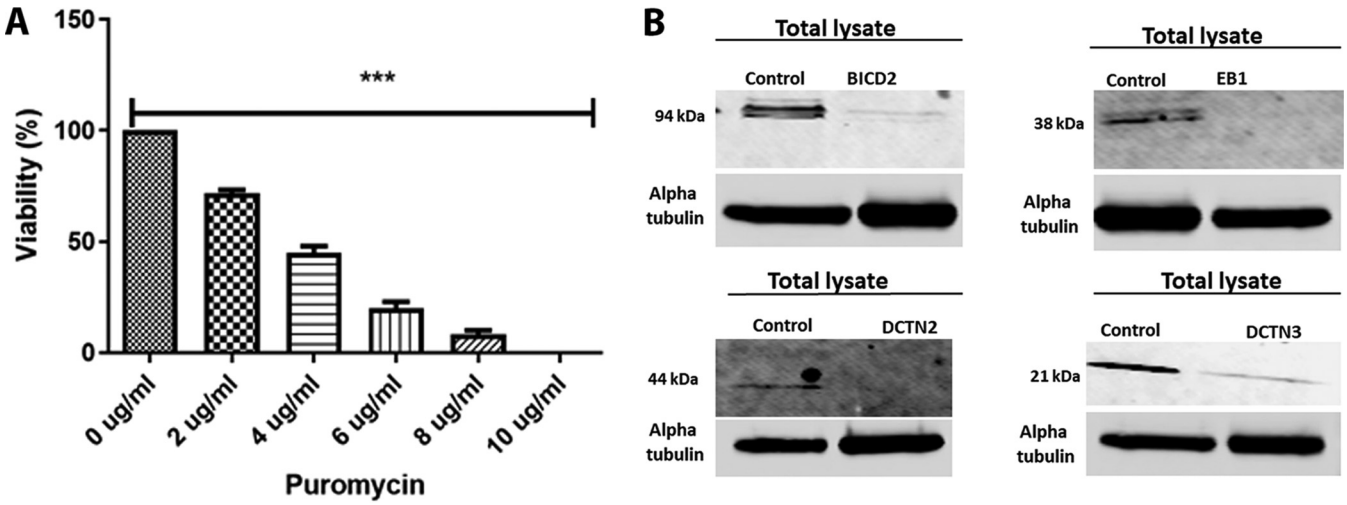

FIG 4 shRNA-mediated silencing of dynein cofactors in the SK-N-SH cell line. (A) Puromycin toxicity assay on SK-N-SH cells. A range of different concentrations (0 to 10 μg/ml) of puromycin was used to determine the appropriate amount of puromycin that is toxic to SK-N-SH cells. ***, $P < 0.001$ versus the no-drug (0 μg/ml)-treated control. Statistical comparison was conducted by GraphPad Prism software using ANOVA with a *post hoc t* test with Bonferroni adjustment. Error bars represent 95% confidence intervals about the means. (B) Lentivirus shRNA (human)-mediated silencing in SK-N-SH cells. The left lanes in each panel show SK-N-SH lysate treated with control shRNA, and the right lanes show lysates treated with shRNA targeted against motor accessory proteins BICD2, EB1, and the dynactin complex (DCTN2 and DCTN3), respectively.

36, 38, 48, 72). To investigate whether viral tegument protein UL37 and the major capsid protein VP5 interact with the dynein intermediate chain, dynactin (DCTN1/p150, and DCTN4/p62), and the microtubule-binding protein EB1 early postinfection, we performed immunoprecipitation assays. Other subunits of dynactins were not investigated due to the lack of antibodies for pulldown assays. Anti-UL37 antibody precipitated DIC and anti-DIC antibody precipitated UL37 from lysates of SK-N-SH HSV-1 (McKrae)-infected cell extracts prepared at 2 hpi (Fig. 7A). Furthermore, colocalization of UL37 and DIC via immunofluorescence assay supported UL37-DIC interaction at an early time postinfection (data not shown). Similarly, immunoprecipitation of the same cellular extracts with anti-VP5 antibody precipitated DCTN1, p62, and EB1, but not DIC (Fig. 7B).

DISCUSSION

HSV-1 enters neuronal axons exclusively via fusion of the viral envelope with axonal membranes, while it can enter into epithelial cells, fibroblasts, and other cells via both fusion at the plasma membrane or via endocytosis after fusion of the viral envelope with endosomal membranes (68, 73). Previously, we reported that the N-terminal 38 amino acids of glycoprotein K (gK) interacts with the amino terminus of gB and modulates gB-mediated membrane fusion, and that this interaction is required for entry via fusion at the plasma membrane in neuronal axons and epithelial cells in cell culture (74–78). Furthermore, we showed that during entry into Vero and SK-N-SH cells, viral glycoprotein B (gB) interacts with Akt and triggers intracellular calcium mobilization. Interaction of gB with phosphorylated Akt, which normally resides in the inner leaflet of the plasma membrane was due to HSV-induced flipping of the inner leaflet of the plasma membrane to the outer side, exposing Akt on cell surfaces (67). Lack of the amino terminus of gK prevented these events to occur and may be responsible for the inability of virions to enter via fusion at the plasma membrane. HSV-1 triggers Akt phosphorylation early times postinfection in both epithelial and proliferating neuronal cell lines (64). Also, Akt phosphorylation was required for virus entry, since the Akt inhibitor miltefosine prevented virus entry (64, 67). Herein, we report that Akt and protein kinase C (PKC) inhibitors block both virus entry and intracellular capsid transport to the nucleus in infected human neuroblastoma cells. HSV-1 infection induced phosphorylation of motor protein dynein via an Akt/PKC-independent pathway, while the

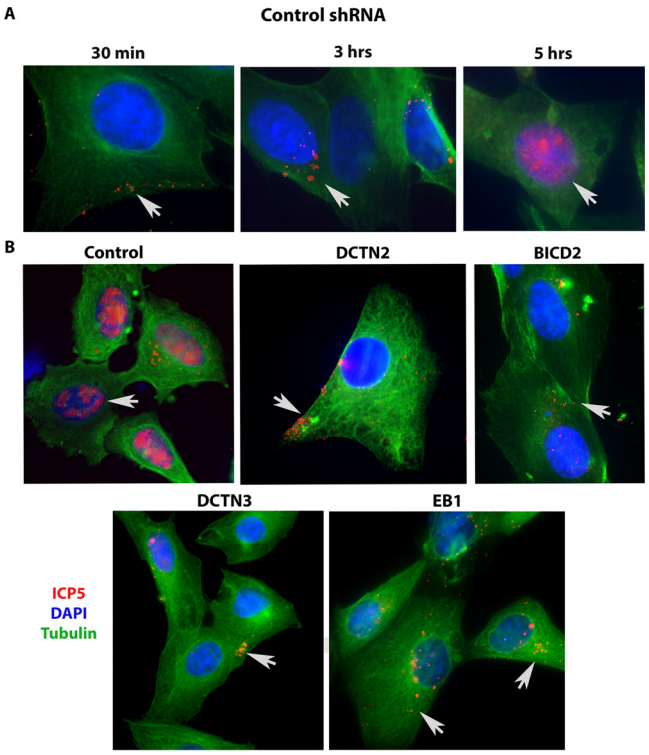

FIG 5 Role of motor accessory proteins in HSV-1 intracellular transport. shRNA-treated SK-N-SH cells were synchronously infected with HSV-1 (McKrae) at an MOI of 20 for 30 min, 3 h, and 5 h at 37°C. Control-shRNA-treated SK-N-SH shows the presence of VP5 (ICP5) in the nucleus at 5 hpi (A). (B) Side-by-side comparison between control shRNA and shRNA against motor accessory protein-treated SK-N-SH cells infected with HSV-1 (McKrae) at an MOI of 20 for 5 h. The 8-well chamber slide was fixed with formalin, permeabilized with methanol, and prepared for fluorescence microscopy. Antibody against VP5 (ICP5) (red) was used, and nuclei were stained with DAPI (blue). Capsids colocalized in the nuclei are visible as purple (red plus blue). Magnification of 60× with oil immersion.

major capsid protein VP5 and the tegument protein UL37 interacted with the dynein motor complex and certain cofactors required for retrograde transport in SK-N-SH cells. These results show that HSV-1 entry and intracellular transport are regulated by viral protein interactions with the dynein protein complex, as well as by modulation of kinase activities other than Akt and PKC (Fig. 8).

Intracellular signaling pathways are regulated during HSV-1 infection. Previously it was shown that HSV-1 triggers activation of MAPK pathways (extracellular signal-regulated kinase 1/2 [ERK1/2], stress-activated protein kinase/Jun N-terminal kinase [SAPK/JNK], and p38) during late times (3 h and 9 h) postinfection (65). Also, it was also reported that the HSV-1 glycoprotein H (gH) alone was sufficient to activate the JNK pathway (79). We report that activation of MAPK pathways by HSV-1 (McKrae) occurs early during infection (15 min postentry) (data not shown). However, virus entry or capsid intracellular transport along microtubules was independent of the MAPK pathways, since a specific MAPK inhibitor did not prevent either HSV-1 (McKrae) entry or capsid transport (data not shown). MAPK activation leads to cell proliferation, differentiation, generation of stress response, and increased cell survival and motility, which may ultimately benefit HSV-1 infection (80). Also, the ERK pathway was reported to play role in the regulation of viral gene expression for SV40, adenovirus, hepatitis B virus, and HIV (81–84). Retrograde transport of nerve growth factor (NGF) within the signaling endosome in mammalian axons is regulated by MAPKs, along with Akt/PI3K and PKC/phospholipase C-γ (PLC-γ) (85). It will be interesting to investigate if HSV-1-induced MAPK activation indirectly regulates other kinases such as Akt or PKC.

The Akt pathway was found to be essential for HSV-1 (McKrae) entry and intracellular

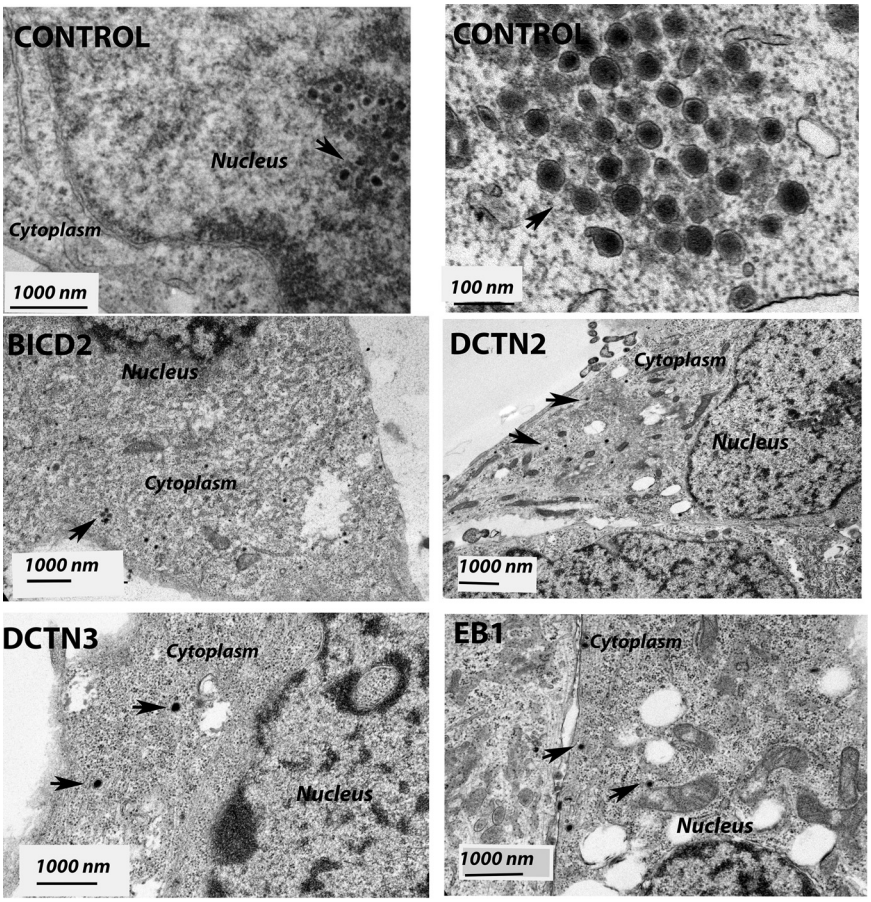

FIG 6 Transmission electron micrograph (TEM) of HSV-1 (McKrae)-infected SK-N-SH cells treated with control, EB1, BICD2, DCTN2, and DCTN3 shRNAs. The knockout SK-N-SH cells were synchronously infected with HSV-1 (McKrae) at an MOI of 20 for 5 h at 37°C. Following infection, cells were fixed and prepared for electron microscopy. SK-N-SH cells treated with control shRNA shows the presence of HSV-1 (McKrae) capsid-like structure in the nucleus. A higher magnification (100 nm) is used for better visibility. Other than the control, HSV-1 (McKrae) capsids were visible only in the cytoplasm, but not in the nucleus of the motor accessory protein knockout SK-N-SH cells. Black arrowheads specify the location of HSV-1 McKrae capsids.

transport in epithelial (Vero) and neuroblastoma (SK-N-SH) cells. Importantly, our results suggest that HSV-1 (McKrae) entry and replication depend on PKC activity. The Akt inhibitor miltofesine is a potent inhibitor of Akt; however, it also inhibits kinase C. Thus, it can be concluded that kinase C is involved in both virus entry and intracellular transport of capsids. Akt directly phosphorylates glycogen synthase kinase (GSK), which regulates microtubule stabilization. Phosphorylation of different microtubule-associated proteins (MAPs) by GSK3 induces accumulation of Tau, which is a characteristic of Alzheimer's disease. GSK3 directly phosphorylates CLIP-170 but not EB1 and destabilize microtubules (86). Therefore, it is possible that Akt and PKC regulate one or more MAPs and restrict HSV-1 capsid loading onto microtubules for transport, as most of the virion capsids were seen at the periphery of the cells in SK-N-SH cells treated with an Akt inhibitor immediately following entry into cells.

Viral activation/phosphorylation of the dynein protein complex. Following entry into the host cell, virion particles can be transported either directly by recruiting cellular motor proteins or indirectly by binding to the cargo of a specific motor protein (26). The major cellular motor protein dynein must be phosphorylated and activated to perform the motor function (9, 14–16, 23). It was shown that HSV-1 capsids require the cellular dynein motor complex for efficient capsid transport toward the nucleus (44).

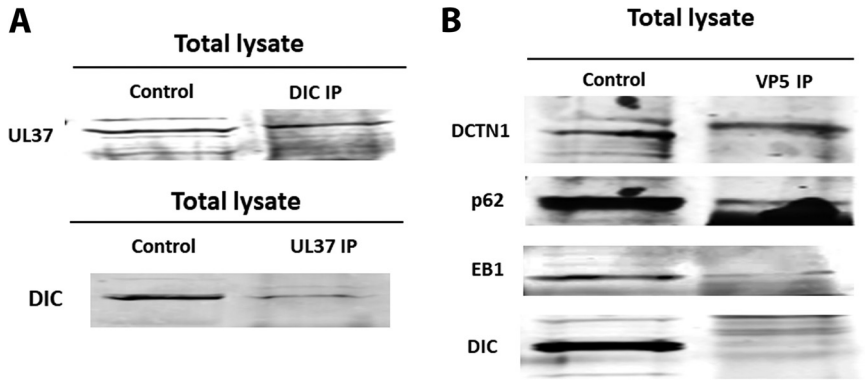

FIG 7 Interactions between HSV-1 capsid/tegument proteins and cellular motor and accessory proteins. (A) Two-way immunoprecipitations (IP) showing UL37 and dynein intermediate-chain (DIC) interaction in HSV-1 (McKrae)-infected SK-N-SH lysates at 2 h postinfection at an MOI of 10. (B) Immunoprecipitation assay showing potential interactions between VP5 and DCTN1, VP5 and p62, and VP5 and EB1 and no interaction between VP5 and DIC proteins. SK-N-SH cells were infected with HSV-1 (McKrae) at an MOI of 10 for an hour, and lysates were prepared with NP-40 lysis buffer with protease inhibitor cocktail. The left lane represents SK-N-SH lysates (control), and the right lane represents lysates immunoprecipitated for HSV-1 VP5 and subsequently probed for dynactin complex (DCTN1 [p150], p62 [DCTN4]), EB1, and DIC.

HSV-1 infection causes rapid dynein phosphorylation (DIC 1B S80A) following fusion/entry, which is not mediated by either Akt or PKC, since treatment with miltefosine, which inhibits both enzymes, did not inhibit dynein phosphorylation. Therefore, dynein must be phosphorylated by a different cellular or viral kinase. It is possible that the viral kinase encoded by the US3 gene, a structural component of the virus inner tegument, may be directly involved in dynein phosphorylation. US3 is one of three tegument proteins that remain attached to the capsid during intracellular capsids transport toward the nucleus, which places US3 in close proximity to the dynein motor machinery. Preliminary data (not shown) also suggest that US3 may interact with DIC. Future work will address whether US3 is involved in dynein phosphorylation and the facilitation of intracellular capsid transport.

Interaction of viral proteins with the dynein protein complex. HSV-1 utilizes dynactin and the EB1 cofactor proteins for transport toward the nucleus along microtubules following entry into host cells (7, 26, 35, 36, 43, 45). The involvement of dynactin in intracellular transport is further supported by the observation that the dynactin cofactor BICD2 is required for efficient intracellular transport, as shown in HIV infection (24). Absence of dynactins DCTN2 and DCTN3, or the EB1 and BICD2 adaptors, significantly reduced HSV-1 transport following entry compared to mock (control shRNA) infection. These results suggest that HSV-1 requires dynein and its accessory proteins for efficient transport of viral capsid toward the nucleus.

In this report, we show for the first time that the major capsid protein VP5 (ICP5) directly interacts with dynactins (DCTN1/p150 and DCTN4/p62) and the EB1 cofactor, which has previously been shown to facilitate HSV-1 transport by helping to load viral capsids onto microtubules (7). EB1 binds to the plus end of microtubules, which is close in proximity to the cell membrane. We assume that capsid loading on microtubules via EB1 occurs immediately after entry through the plasma membrane. EB1 may detach after loading of the capsids onto microtubules or may remain attached to the capsid motor complex during the transport. Other plus-end binding proteins may also be involved in this process. The tegument protein UL37 interacts with the dynein intermediate chain (DIC), which is phosphorylated after HSV-1 infection. It is not clear at this point whether DIC phosphorylation is required for interaction with the UL37 protein. Since dynactins and the dynein motor complex work synergistically in retrograde cellular transport, binding of VP5 to dynactins and EB1 and binding of UL37 to dynein

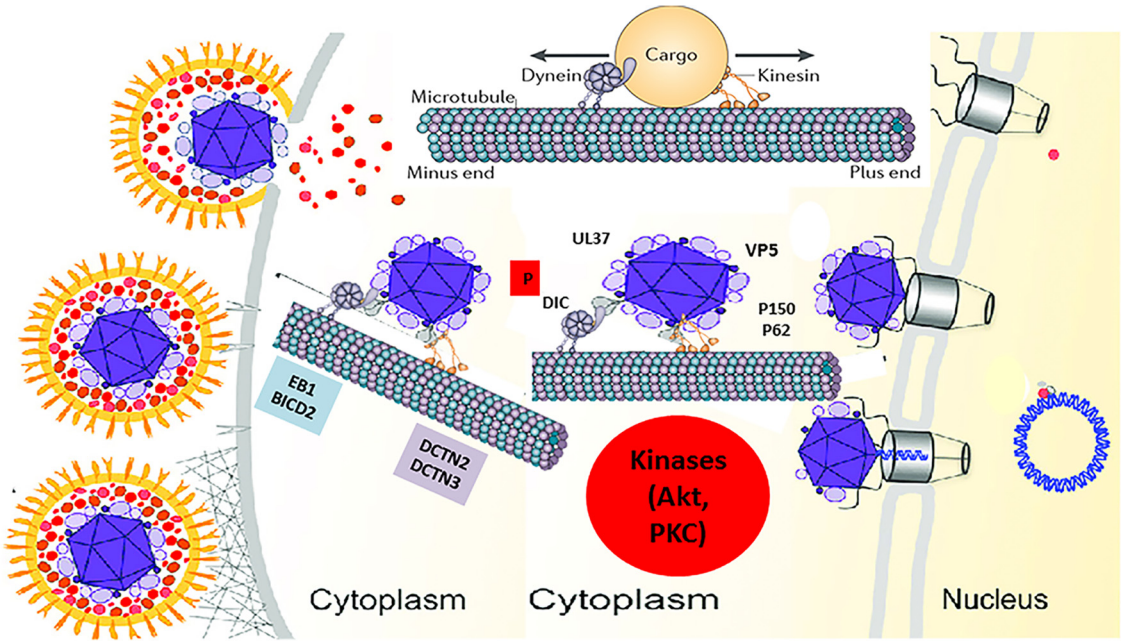

FIG 8 Model of HSV-1 transport into host cells. The schematic shows the molecules and intracellular signaling, which may be involved in intracellular capsid transport. Following entry into host cells, HSV-1 (McKrae) activates/phosphorylates the dynein motor and the Akt and MAPK pathways (data not shown). The major capsid protein VP5 (ICP5) and the inner tegument protein UL37 recruit the dynein motor and other accessory proteins, such as BICD2, EB1, and the dynactin complex (DCTN) to facilitate retrograde transport of virion capsids. Akt and PKC activities are required for efficient entry and transport along the microtubules toward the nucleus, where the virus replicates its DNA. (Adapted from reference 87.)

may stabilize the overall virus-motor interaction facilitating intracellular transport of capsid toward the nucleus.

Overall, these results suggest that virus entry and intracellular capsid transport require the action of cellular and viral kinases. These cellular kinases may regulate interactions of viral tegument and capsid proteins with the dynein motor machinery, including dynactin and its accessory cofactors. Identification of these kinases and the specific protein-protein interactions that are involved may provide new ways to prevent both virus entry and intracellular transport.

MATERIALS AND METHODS

Cells and viruses. African green monkey kidney cells (Vero; ATCC) and human neuroblastoma cells (SK-N-SH; ATCC) were used for most of the experiments. Vero cells were grown in filter-sterilized Dulbecco's modified Eagle's media (DMEM) supplemented with 10% fetal bovine serum (FBS) and 0.2% Primocin (Invitrogen, Inc., Carlsbad, CA). SK-N-SH cells were grown in filter-sterilized Eagle's minimal essential medium (EMEM) supplemented with 10% FBS and 0.2% Primocin. All cells were incubated at 37°C with 5% CO_2. A pathogenic strain of HSV-1 expressing green fluorescent protein (McKrae-GFP) was used throughout the experiments.

Antibodies and reagents. Antibodies against α-tubulin, HSV-1 ICP5, intermediate dynein chain (DIC), dynein heavy chain (DHC), dynactin 1/p150 (DCTN 1), dynactin 2/dynamitin (DCTN 2), and dynactin 3 (DCTN 3) were purchased from Abcam, Inc., Cambridge, MA. Antibodies against end binding protein 1 (EB1) and VP5 were purchased from Santa Cruz Biotechnology, Dallas, TX. The HSV-1 UL37 antibody was a gift from Frank J. Jenkins, University of Pittsburgh Cancer Institute. Antibody against phosphorylated DIC was a gift from Kevin Pfister's laboratory, University of Virginia. A MAPK family antibody sampler kit was obtained from Cell Signaling Technologies, Danvers, MA. The Akt inhibitor miltefosine and the MAPK inhibitor PD 98059 were purchased from Santa Cruz Biotechnology, Dallas, TX, and the PKC inhibitors STS and Gouml were obtained from Abcam, Inc., Cambridge, MA.

Immunoprecipitation and immunoblot assays. SK-N-SH cells were infected with HSV-1 (McKrae) at an MOI of 10. At 1 h postinfection (hpi), the infected cells were lysed with NP-40 cell lysis buffer (Life Technologies, Carlsbad, CA) supplemented with protease inhibitor tablets (Sigma, Inc., St. Louis, MO). The samples were centrifuged at 13,000 rpm for 10 min at 4°C. The supernatants were then used for immunoprecipitation. Proteins from virus-infected cells were immunoprecipitated using protein G magnetic Dynabeads according to the manufacturer's instructions (Invitrogen, Carlsbad, CA). Briefly, the beads were bound to their respective antibodies and placed on a nutator for 10 min, followed by the

addition of cell lysates. The lysate-bead mixture was kept on the nutator for 10 min at room temperature and subsequently washed three times with 1× phosphate-buffered saline (PBS). The protein was eluted from the magnetic beads in 40 μl of elution buffer and used for immunoblot assays. Sample buffer containing 5% β-mercaptoethanol was added to the samples, and then they were heated at 55°C for 15 min. Proteins were resolved in a 4 to 20% SDS-PAGE gel and immobilized on either nitrocellulose or polyvinylidene difluoride (PVDF) membranes. For Western immunoblots, subconfluent SK-N-SH cells were infected with the indicated viruses at an MOI of 10 for different time points, as mentioned above. The cells were similarly lysed with the NP-40 lysis buffer, and the lysate was used for Western immunoblots. Immunoblot assays were carried out using rabbit anti-Akt-1 S473 antibody (Millipore, Burlington, MA), rabbit anti-Akt 1/2/3 antibody (Millipore, Burlington, MA), rabbit anti-MAPK family antibodies (Cell Signaling Technologies, Danvers, MA), rabbit anti-dynein intermediate-chain phosphorylation (DIC 1B S80A) antibody (from the laboratory of Kevin Pfister), mouse anti-DIC antibody (Abcam plc, Cambridge, MA), horseradish peroxidase (HRP)-conjugated goat anti-mouse antibodies against the light chain (Fab) and heavy chain (Fc) (Abcam, plc, Cambridge, MA), and HRP-conjugated goat anti-rabbit antibody (Abcam, plc, Cambridge, MA).

Lentivirus shRNA-mediated gene silencing. shRNAs targeting dynein heavy chain (DHC), BICD2, dynactin 2 (DCTN 2), dynactin 3 (DCTN 3), and end binding protein 1 (EB1) were used and delivered via lentiviral vectors in SK-N-SH cells. The level of expression of these proteins was detected by Western blot analysis of lysates of transduced cells. Gene silencing by shRNA was performed according to the protocol provided by Santa Cruz Biotechnology. Briefly, cells were grown in complete medium (with 10% FBS and 0.2% Primocin) in 12-well plates. Lentivirus transduction was performed when cell monolayers were approximately 50% confluent. To increase the binding between the pseudoviral capsids and the cellular membrane, Polybrene (sc-134220) was used at a final concentration of 5 μg/ml of complete growth medium. The medium was removed and replaced with 1 ml of Polybrene medium per well. Lentiviral particles were thawed at room temperature and mixed gently before use. The cells were transduced by adding shRNA lentiviral particles to the culture. Following overnight incubation at 37°C, the growth medium was removed and replaced with 1 ml of complete medium without Polybrene. To select stable clones expressing the shRNA, cells were split 1:3 to 1:5 depending on the cell type, and puromycin hydrochloride was used as a selection agent. Prior to transduction, a puromycin titration was done to determine the sufficient concentration to kill the nontransduced cells. To kill nontransduced cells, puromycin was used at concentrations of 15 μg/ml for Vero cells and 10 μg/ml for SK-N-SH cells.

Retrograde transport assay. SK-N-SH cells were grown in eight-well chamber slides and serum starved overnight. Cells were then adsorbed with HSV-1 (McKrae) at 4°C at an MOI of 20. The slides were then shifted to 37°C for 15 min and then washed with a low-pH buffer. The cells were treated with the inhibitors of choice for 5 h at 37°C. Subsequently, the slides were fixed in formalin and permeabilized with ice-cold methanol followed by blocking with 10% goat serum. Antibody against ICP5 was used to detect viral capsid transport to the nucleus, which also was stained with DAPI (4′,6-diamidino-2-phenylindole). Images were taken using a 60× objective (oil immersion) on a fluorescence microscope.

Drug toxicity/cell viability assay. Vero cells were grown in 12-well plates and serum starved overnight before treatment. Drugs were dissolved in dimethyl sulfoxide (DMSO), and the dilutions were made in DMEM without serum. Cells were treated with different dilutions of drugs and incubated at 37°C for 24 h. Each dilution was tested in triplicate. The percentage of live cells was quantified using trypan blue. The counts from treated wells were compared with those of the nontreated wells.

Statistical analyses. Statistical analyses were performed by using analysis of variance (ANOVA); Student's *t* test and *P* values of <0.05 were considered significant. Bonferroni adjustments were applied for multiple comparisons between control and treatment groups. All analyses were performed using GraphPad Prism (version 5) software (GraphPad Software, San Diego, CA, USA).

ACKNOWLEDGMENTS

The work was supported by the LSU Division of Biotechnology & Molecular Medicine, by a Governor's Biotechnology Initiative grant (to K.G.K.), and by Cores of the Center for Experimental Infectious Disease Research (CEIDR), funded by NIH, NIGMS, and grant P30GM110670.

We thank Kevin Pfister for providing the phospho-dynein antibody, Xiaochu Wu for assistance with electron microscopy, and Peter Mottram for helping with fluorescent microscopy.

REFERENCES

1. Evans RD, Robinson C, Briggs DA, Tooth DJ, Ramalho JS, Cantero M, Montoliu L, Patel S, Sviderskaya EV, Hume AN. 2014. Myosin-Va and dynamic actin oppose microtubules to drive long-range organelle transport. Curr Biol 24:1743–1750. https://doi.org/10.1016/j.cub.2014.06.019.
2. Cramer L. 2008. Organelle transport: dynamic actin tracks for myosin motors. Curr Biol 18:R1066–R1068. https://doi.org/10.1016/j.cub.2008.09.048.
3. Schuh M. 2011. An actin-dependent mechanism for long-range vesicle transport. Nat Cell Biol 13:1431–1436. https://doi.org/10.1038/ncb2353.
4. Barlan K, Gelfand VI. 2017. Microtubule-based transport and the distribution, tethering, and organization of organelles. Cold Spring Harb Perspect Biol 9:a025817. https://doi.org/10.1101/cshperspect.a025817.
5. Kapitein LC, Hoogenraad CC. 2011. Which way to go? Cytoskeletal organization and polarized transport in neurons. Mol Cell Neurosci 46:9–20. https://doi.org/10.1016/j.mcn.2010.08.015.
6. Jiang K, Akhmanova A. 2011. Microtubule tip-interacting proteins: a view from both ends. Curr Opin Cell Biol 23:94–101. https://doi.org/10.1016/j.ceb.2010.08.008.
7. Jovasevic V, Naghavi MH, Walsh D. 2015. Microtubule plus end-associated

CLIP-170 initiates HSV-1 retrograde transport in primary human cells. J Cell Biol 211:323–337. https://doi.org/10.1083/jcb.201505123.
8. Honnappa S, Gouveia SM, Weisbrich A, Damberger FF, Bhavesh NS, Jawhari H, Grigoriev I, van Rijssel FJ, Buey RM, Lawera A, Jelesarov I, Winkler FK, Wuthrich K, Akhmanova A, Steinmetz MO. 2009. An EB1-binding motif acts as a microtubule tip localization signal. Cell 138:366–376. https://doi.org/10.1016/j.cell.2009.04.065.
9. Hook P, Vallee RB. 2006. The dynein family at a glance. J Cell Sci 119:4369–4371. https://doi.org/10.1242/jcs.03176.
10. Pfister KK, Fisher EMC, Gibbons IR, Hays TS, Holzbaur ELF, McIntosh JR, Porter ME, Schroer TA, Vaughan KT, Witman GB, King SM, Vallee RB. 2005. Cytoplasmic dynein nomenclature. J Cell Biol 171:411–413. https://doi.org/10.1083/jcb.200508078.
11. Pfister KK, Shah PR, Hummerich H, Russ A, Cotton J, Annuar AA, King SM, Fisher EM. 2006. Genetic analysis of the cytoplasmic dynein subunit families. PLoS Genet 2:e1. https://doi.org/10.1371/journal.pgen.0020001.
12. Nyarko A, Barbar E. 2011. Light chain-dependent self-association of dynein intermediate chain. J Biol Chem 286:1556–1566. https://doi.org/10.1074/jbc.M110.171686.
13. Makokha M, Hare M, Li M, Hays T, Barbar E. 2002. Interactions of cytoplasmic dynein light chains Tctex-1 and LC8 with the intermediate chain IC74. Biochemistry 41:4302–4311. https://doi.org/10.1021/bi011970h.
14. Liu JJ. 2017. Regulation of dynein-dynactin-driven vesicular transport. Traffic 18:336–347. https://doi.org/10.1111/tra.12475.
15. Olenick MA, Holzbaur ELF. 2019. Dynein activators and adaptors at a glance. J Cell Sci 132:jcs227132. https://doi.org/10.1242/jcs.227132.
16. Chowdhury S, Ketcham SA, Schroer TA, Lander GC. 2015. Structural organization of the dynein-dynactin complex bound to microtubules. Nat Struct Mol Biol 22:345–347. https://doi.org/10.1038/nsmb.2996.
17. King SJ, Brown CL, Maier KC, Quintyne NJ, Schroer TA. 2003. Analysis of the dynein-dynactin interaction in vitro and in vivo. Mol Biol Cell 14:5089–5097. https://doi.org/10.1091/mbc.e03-01-0025.
18. Karki S, Holzbaur EL. 1995. Affinity chromatography demonstrates a direct binding between cytoplasmic dynein and the dynactin complex. J Biol Chem 270:28806–28811. https://doi.org/10.1074/jbc.270.48.28806.
19. Urnavicius L, Zhang K, Diamant AG, Motz C, Schlager MA, Yu M, Patel NA, Robinson CV, Carter AP. 2015. The structure of the dynactin complex and its interaction with dynein. Science 347:1441–1446. https://doi.org/10.1126/science.aaa4080.
20. Will L, Portegies S, van Schelt J, van Luyk M, Jaarsma D, Hoogenraad CC. 2019. Dynein activating adaptor BICD2 controls radial migration of upper-layer cortical neurons in vivo. Acta Neuropathol Commun 7:162. https://doi.org/10.1186/s40478-019-0827-y.
21. Splinter D, Razafsky DS, Schlager MA, Serra-Marques A, Grigoriev I, Demmers J, Keijzer N, Jiang K, Poser I, Hyman AA, Hoogenraad CC, King SJ, Akhmanova A. 2012. BICD2, dynactin, and LIS1 cooperate in regulating dynein recruitment to cellular structures. Mol Biol Cell 23:4226–4241. https://doi.org/10.1091/mbc.E12-03-0210.
22. Indran SV, Ballestas ME, Britt WJ. 2010. Bicaudal D1-dependent trafficking of human cytomegalovirus tegument protein pp150 in virus-infected cells. J Virol 84:3162–3177. https://doi.org/10.1128/JVI.01776-09.
23. Kardon JR, Vale RD. 2009. Regulators of the cytoplasmic dynein motor. Nat Rev Mol Cell Biol 10:854–865. https://doi.org/10.1038/nrm2804.
24. Carnes SK, Zhou J, Aiken C. 2018. HIV-1 engages a dynein-dynactin-BICD2 complex for infection and transport to the nucleus. J Virol 92:e00358-18. https://doi.org/10.1128/JVI.00358-18.
25. Hirano M, Muto M, Sakai M, Kondo H, Kobayashi S, Kariwa H, Yoshii K. 2017. Dendritic transport of tick-borne flavivirus RNA by neuronal granules affects development of neurological disease. Proc Natl Acad Sci U S A 114:9960–9965. https://doi.org/10.1073/pnas.1704454114.
26. Dohner K, Sodeik B. 2005. The role of the cytoskeleton during viral infection. Curr Top Microbiol Immunol 285:67–108. https://doi.org/10.1007/3-540-26764-6_3.
27. Gluska S, Zahavi EE, Chein M, Gradus T, Bauer A, Finke S, Perlson E. 2014. Rabies virus hijacks and accelerates the p75NTR retrograde axonal transport machinery. PLoS Pathog 10:e1004348. https://doi.org/10.1371/journal.ppat.1004348.
28. Kramer T, Enquist LW. 2012. Alphaherpesvirus infection disrupts mitochondrial transport in neurons. Cell Host Microbe 11:504–514. https://doi.org/10.1016/j.chom.2012.03.005.
29. Dodding MP, Way M. 2011. Coupling viruses to dynein and kinesin-1. EMBO J 30:3527–3539. https://doi.org/10.1038/emboj.2011.283.
30. Ravindran MS, Spriggs CC, Verhey KJ, Tsai B. 2018. Dynein engages and disassembles cytosol-localized simian virus 40 to promote infection. J Virol 92:e00353-18. https://doi.org/10.1128/JVI.00353-18.
31. Antinone SE, Smith GA. 2010. Retrograde axon transport of herpes simplex virus and pseudorabies virus: a live-cell comparative analysis. J Virol 84:1504–1512. https://doi.org/10.1128/JVI.02029-09.
32. Douglas MW, Diefenbach RJ, Homa FL, Miranda-Saksena M, Rixon FJ, Vittone V, Byth K, Cunningham AL. 2004. Herpes simplex virus type 1 capsid protein VP26 interacts with dynein light chains RP3 and Tctex1 and plays a role in retrograde cellular transport. J Biol Chem 279:28522–28530. https://doi.org/10.1074/jbc.M311671200.
33. Miranda-Saksena M, Denes CE, Diefenbach RJ, Cunningham AL. 2018. Infection and transport of herpes simplex virus type 1 in neurons: role of the cytoskeleton. Viruses 10:92. https://doi.org/10.3390/v10020092.
34. Luby-Phelps K. 1994. Physical properties of cytoplasm. Curr Opin Cell Biol 6:3–9. https://doi.org/10.1016/0955-0674(94)90109-0.
35. Richards AL, Sollars PJ, Pitts JD, Stults AM, Heldwein EE, Pickard GE, Smith GA. 2017. The pUL37 tegument protein guides alpha-herpesvirus retrograde axonal transport to promote neuroinvasion. PLoS Pathog 13:e1006741. https://doi.org/10.1371/journal.ppat.1006741.
36. Radtke K, Kieneke D, Wolfstein A, Michael K, Steffen W, Scholz T, Karger A, Sodeik B. 2010. Plus- and minus-end directed microtubule motors bind simultaneously to herpes simplex virus capsids using different inner tegument structures. PLoS Pathog 6:e1000991. https://doi.org/10.1371/journal.ppat.1000991.
37. Kelly BJ, Fraefel C, Cunningham AL, Diefenbach RJ. 2009. Functional roles of the tegument proteins of herpes simplex virus type 1. Virus Res 145:173–186. https://doi.org/10.1016/j.virusres.2009.07.007.
38. Buch A, Muller O, Ivanova L, Dohner K, Bialy D, Bosse JB, Pohlmann A, Binz A, Hegemann M, Nagel CH, Koltzenburg M, Viejo-Borbolla A, Rosenhahn B, Bauerfeind R, Sodeik B. 2017. Inner tegument proteins of herpes simplex virus are sufficient for intracellular capsid motility in neurons but not for axonal targeting. PLoS Pathog 13:e1006813. https://doi.org/10.1371/journal.ppat.1006813.
39. Koenigsberg AL, Heldwein EE. 2018. The dynamic nature of the conserved tegument protein UL37 of herpesviruses. J Biol Chem 293:15827–15839. https://doi.org/10.1074/jbc.RA118.004481.
40. Dai X, Zhou ZH. 2018. Structure of the herpes simplex virus 1 capsid with associated tegument protein complexes. Science 360:eaao7298. https://doi.org/10.1126/science.aao7298.
41. Ivanova L, Buch A, Döhner K, Pohlmann A, Binz A, Prank U, Sandbaumhüter M, Bauerfeind R, Sodeik B. 2016. Conserved tryptophan motifs in the large tegument protein pUL36 are required for efficient secondary envelopment of herpes simplex virus capsids. J Virol 90:5368–5383. https://doi.org/10.1128/JVI.03167-15.
42. Sandbaumhüter M, Döhner K, Schipke J, Binz A, Pohlmann A, Sodeik B, Bauerfeind R. 2013. Cytosolic herpes simplex virus capsids not only require binding inner tegument protein pUL36 but also pUL37 for active transport prior to secondary envelopment. Cell Microbiol 15:248–269. https://doi.org/10.1111/cmi.12075.
43. Kramer T, Enquist LW. 2013. Directional spread of alphaherpesviruses in the nervous system. Viruses 5:678–707. https://doi.org/10.3390/v5020678.
44. Dohner K, Wolfstein A, Prank U, Echeverri C, Dujardin D, Vallee R, Sodeik B. 2002. Function of dynein and dynactin in herpes simplex virus capsid transport. Mol Biol Cell 13:2795–2809. https://doi.org/10.1091/mbc.01-07-0348.
45. Zaichick SV, Bohannon KP, Hughes A, Sollars PJ, Pickard GE, Smith GA. 2013. The herpesvirus VP1/2 protein is an effector of dynein-mediated capsid transport and neuroinvasion. Cell Host Microbe 13:193–203. https://doi.org/10.1016/j.chom.2013.01.009.
46. Desfarges S, Salin B, Calmels C, Andreola ML, Parissi V, Fournier M. 2009. HIV-1 integrase trafficking in S. cerevisiae: a useful model to dissect the microtubule network involvement of viral protein nuclear import. Yeast 26:39–54. https://doi.org/10.1002/yea.1651.
47. Dharan A, Opp S, Abdel-Rahim O, Keceli SK, Imam S, Diaz-Griffero F, Campbell EM. 2017. Bicaudal D2 facilitates the cytoplasmic trafficking and nuclear import of HIV-1 genomes during infection. Proc Natl Acad Sci U S A 114:E10707–E10716. https://doi.org/10.1073/pnas.1712033114.
48. Bremner KH, Scherer J, Yi J, Vershinin M, Gross SP, Vallee RB. 2009. Adenovirus transport via direct interaction of cytoplasmic dynein with the viral capsid hexon subunit. Cell Host Microbe 6:523–535. https://doi.org/10.1016/j.chom.2009.11.006.
49. Pines J. 1994. Protein kinases and cell cycle control. Semin Cell Biol 5:399–408. https://doi.org/10.1006/scel.1994.1047.
50. Ardito F, Giuliani M, Perrone D, Troiano G, Lo Muzio L. 2017. The crucial role

of protein phosphorylation in cell signaling and its use as targeted therapy. Int J Mol Med 40:271–280. https://doi.org/10.3892/ijmm.2017.3036.
51. MacCorkle RA, Tan TH. 2005. Mitogen-activated protein kinases in cell-cycle control. Cell Biochem Biophys 43:451–461. https://doi.org/10.1385/CBB:43:3:451.
52. Lu Z, Xu S. 2006. ERK1/2 MAP kinases in cell survival and apoptosis. IUBMB Life 58:621–631. https://doi.org/10.1080/15216540600957438.
53. Yin H, Stojanovic A, Hay N, Du X. 2008. The role of Akt in the signaling pathway of the glycoprotein Ib-IX induced platelet activation. Blood 111:658–665. https://doi.org/10.1182/blood-2007-04-085514.
54. Karunakaran D, Kockx M, Owen DM, Burnett JR, Jessup W, Kritharides L. 2013. Protein kinase C controls vesicular transport and secretion of apolipoprotein E from primary human macrophages. J Biol Chem 288:5186–5197. https://doi.org/10.1074/jbc.M112.428961.
55. de Jong AP, Meijer M, Saarloos I, Cornelisse LN, Toonen RF, Sorensen JB, Verhage M. 2016. Phosphorylation of synaptotagmin-1 controls a post-priming step in PKC-dependent presynaptic plasticity. Proc Natl Acad Sci U S A 113:5095–5100. https://doi.org/10.1073/pnas.1522927113.
56. Job C, Lagnado L. 1998. Calcium and protein kinase C regulate the actin cytoskeleton in the synaptic terminal of retinal bipolar cells. J Cell Biol 143:1661–1672. https://doi.org/10.1083/jcb.143.6.1661.
57. Gibbs KL, Greensmith L, Schiavo G. 2015. Regulation of axonal transport by protein kinases. Trends Biochem Sci 40:597–610. https://doi.org/10.1016/j.tibs.2015.08.003.
58. Chan WK, Dickerson A, Ortiz D, Pimenta AF, Moran CM, Motil J, Snyder SJ, Malik K, Pant HC, Shea TB. 2004. Mitogen-activated protein kinase regulates neurofilament axonal transport. J Cell Sci 117:4629–4642. https://doi.org/10.1242/jcs.01135.
59. Colin E, Zala D, Liot G, Rangone H, Borrell-Pages M, Li XJ, Saudou F, Humbert S. 2008. Huntingtin phosphorylation acts as a molecular switch for anterograde/retrograde transport in neurons. EMBO J 27:2124–2134. https://doi.org/10.1038/emboj.2008.133.
60. Ozsarac N, Weible M, II, Reynolds AJ, Hendry IA. 2003. Activation of protein kinase C inhibits retrograde transport of neurotrophins in mice. J Neurosci Res 72:203–210. https://doi.org/10.1002/jnr.10568.
61. Morfini G, Pigino G, Opalach K, Serulle Y, Moreira JE, Sugimori M, Llinas RR, Brady ST. 2007. 1-Methyl-4-phenylpyridinium affects fast axonal transport by activation of caspase and protein kinase C. Proc Natl Acad Sci U S A 104:2442–2447. https://doi.org/10.1073/pnas.0611231104.
62. Gao FJ, Hebbar S, Gao XA, Alexander M, Pandey JP, Walla MD, Cotham WE, King SJ, Smith DS. 2015. GSK-3β phosphorylation of cytoplasmic dynein reduces Ndel1 binding to intermediate chains and alters dynein motility. Traffic 16:941–961. https://doi.org/10.1111/tra.12304.
63. Le Grand M, Rovini A, Bourgarel-Rey V, Honore S, Bastonero S, Braguer D, Carre M. 2014. ROS-mediated EB1 phosphorylation through Akt/GSK3 beta pathway: implication in cancer cell response to microtubule-targeting agents. Oncotarget 5:3408–3423. https://doi.org/10.18632/oncotarget.1982.
64. Cheshenko N, Trepanier JB, Stefanidou M, Buckley N, Gonzalez P, Jacobs W, Herold BC. 2013. HSV activates Akt to trigger calcium release and promote viral entry: novel candidate target for treatment and suppression. FASEB J 27:2584–2599. https://doi.org/10.1096/fj.12-220285.
65. Zachos G, Clements B, Conner J. 1999. Herpes simplex virus type 1 infection stimulates p38/c-Jun N-terminal mitogen-activated protein kinase pathways and activates transcription factor AP-1. J Biol Chem 274:5097–5103. https://doi.org/10.1074/jbc.274.8.5097.
66. Hamada K, Maeda Y, Mizutani A, Okada S. 2019. The phosphatidylinositol 3-kinase p110 alpha/PTEN signaling pathway is crucial for HIV-1 entry. Biol Pharm Bull 42:130–138. https://doi.org/10.1248/bpb.b18-00801.
67. Musarrat F, Jambunathan N, Rider PJF, Chouljenko VN, Kousoulas KG. 2018. The amino terminus of herpes simplex virus 1 glycoprotein K (gK) is required for gB binding to Akt, release of intracellular calcium, and fusion of the viral envelope with plasma membranes. J Virol 92:e01842-17. https://doi.org/10.1128/JVI.01842-17.
68. Nicola AV, Straus SE. 2004. Cellular and viral requirements for rapid endocytic entry of herpes simplex virus. J Virol 78:7508–7517. https://doi.org/10.1128/JVI.78.14.7508-7517.2004.
69. Scherer J, Yi JL, Vallee RB. 2014. PKA-dependent dynein switching from lysosomes to adenovirus: a novel form of host-virus competition. J Cell Biol 205:163–177. https://doi.org/10.1083/jcb.201307116.
70. Suomalainen M, Nakano MY, Boucke K, Keller S, Greber UF. 2001. Adenovirus-activated PKA and p38/MAPK pathways boost microtubule-mediated nuclear targeting of virus. EMBO J 20:1310–1319. https://doi.org/10.1093/emboj/20.6.1310.
71. Elliott G, O'Hare P. 1998. Herpes simplex virus type 1 tegument protein VP22 induces the stabilization and hyperacetylation of microtubules. J Virol 72:6448–6455. https://doi.org/10.1128/JVI.72.8.6448-6455.1998.
72. Tan GS, Preuss MA, Williams JC, Schnell MJ. 2007. The dynein light chain 8 binding motif of rabies virus phosphoprotein promotes efficient viral transcription. Proc Natl Acad Sci U S A 104:7229–7234. https://doi.org/10.1073/pnas.0701397104.
73. Rider PJF, Coghill LM, Naderi M, Brown JM, Brylinski M, Kousoulas KG. 2019. Identification and visualization of functionally important domains and residues in herpes simplex virus glycoprotein K (gK) using a combination of phylogenetics and protein modeling. Sci Rep 9:14625. https://doi.org/10.1038/s41598-019-50490-9.
74. Chouljenko VN, Iyer AV, Chowdhury S, Chouljenko DV, Kousoulas KG. 2009. The amino terminus of herpes simplex virus type 1 glycoprotein K (gK) modulates gB-mediated virus-induced cell fusion and virion egress. J Virol 83:12301–12313. https://doi.org/10.1128/JVI.01329-09.
75. Chouljenko VN, Iyer AV, Chowdhury S, Kim J, Kousoulas KG. 2010. The herpes simplex virus type 1 UL20 protein and the amino terminus of glycoprotein K (gK) physically interact with gB. J Virol 84:8596–8606. https://doi.org/10.1128/JVI.00298-10.
76. David AT, Baghian A, Foster TP, Chouljenko VN, Kousoulas KG. 2008. The herpes simplex virus type 1 (HSV-1) glycoprotein K (gK) is essential for viral corneal spread and neuroinvasiveness. Curr Eye Res 33:455–467. https://doi.org/10.1080/02713680802130362.
77. David AT, Saied A, Charles A, Subramanian R, Chouljenko VN, Kousoulas KG. 2012. A herpes simplex virus 1 (McKrae) mutant lacking the glycoprotein K gene is unable to infect via neuronal axons and egress from neuronal cell bodies. mBio 3:e00144-12. https://doi.org/10.1128/mBio.00144-12.
78. Saied AA, Chouljenko VN, Subramanian R, Kousoulas KG. 2014. A replication competent HSV-1(McKrae) with a mutation in the amino-terminus of glycoprotein K (gK) is unable to infect mouse trigeminal ganglia after cornea infection. Curr Eye Res 39:596–603. https://doi.org/10.3109/02713683.2013.855238.
79. Galdiero S, Vitiello M, D'Isanto M, Di Niola E, Peluso L, Raieta K, Pedone C, Galdiero M, Benedetti E. 2004. Induction of signaling pathways by herpes simplex virus type 1 through glycoprotein H peptides. Biopolymers 76:494–502. https://doi.org/10.1002/bip.20162.
80. Cargnello M, Roux PP. 2011. Activation and function of the MAPKs and their substrates, the MAPK-activated protein kinases. Microbiol Mol Biol Rev 75:50–83. https://doi.org/10.1128/MMBR.00031-10.
81. Barnabas S, Andrisani OM. 2000. Different regions of hepatitis B virus X protein are required for enhancement of bZip-mediated transactivation versus transrepression. J Virol 74:83–90. https://doi.org/10.1128/jvi.74.1.83-90.2000.
82. Dangoria NS, Breau WC, Anderson HA, Cishek DM, Norkin LC. 1996. Extracellular simian virus 40 induces an ERK/MAP kinase-independent signalling pathway that activates primary response genes and promotes virus entry. J Gen Virol 77:2173–2182. https://doi.org/10.1099/0022-1317-77-9-2173.
83. Fleta-Soriano E, Martinez JP, Hinkelmann B, Gerth K, Washausen P, Diez J, Frank R, Sasse F, Meyerhans A. 2014. The myxobacterial metabolite ratjadone A inhibits HIV infection by blocking the Rev/CRM1-mediated nuclear export pathway. Microb Cell Fact 13:17. https://doi.org/10.1186/1475-2859-13-17.
84. Wu W, Booth JL, Duggan ES, Patel KB, Coggeshall KM, Metcalf JP. 2010. Human lung innate immune cytokine response to adenovirus type 7. J Gen Virol 91:1155–1163. https://doi.org/10.1099/vir.0.017905-0.
85. Ito K, Enomoto H. 2016. Retrograde transport of neurotrophic factor signaling: implications in neuronal development and pathogenesis. J Biochem 160:77–85. https://doi.org/10.1093/jb/mvw037.
86. Buttrick GJ, Wakefield JG. 2008. PI3-K and GSK-3: Akt-ing together with microtubules. Cell Cycle 7:2621–2625. https://doi.org/10.4161/cc.7.17.6514.
87. Ralph M, Bednarchik M, Tomer E, Rafael D, Zargarian S, Gerlic M, Kobiler O. 2017. Promoting simultaneous onset of viral gene expression among cells infected with herpes simplex virus-1. Front Microbiol 8:2152. https://doi.org/10.3389/fmicb.2017.02152.